Propagation of Chirality in Mixtures of Natural and Enantiomeric DNA Oligomers

Marina Rossi,[1] Giuliano Zanchetta,[1] Sven Klussmann,[2] Noel A. Clark,[3] and Tommaso Bellini[1]

[1]*Dipartimento di Biotecnologie Mediche e Medicina Traslazionale, Università degli Studi di Milano, via Fratelli Cervi 93, I-20090 Segrate (MI), Italy*

[2]*NOXXON Pharma AG, Max-Dohrn-Strasse 8-10, 10589 Berlin, Germany*

[3]*Department of Physics and Liquid Crystal Materials Research Center, University of Colorado, Boulder, Colorado 80309-0390, USA*

(Received 15 November 2012; published 7 March 2013)

Concentrated solutions of ultrashort duplex-forming DNA oligomers may develop various forms of liquid crystal ordering among which is the chiral nematic phase, characterized by a macroscopic helical precession of molecular orientation. The specifics of how chirality propagates from the molecular to the mesoscale is still unclear, both in general and in the case of DNA-based liquid crystals. We have here investigated the onset of nematic ordering and its chiral character in mixtures of natural *D*-DNA oligomers forming right-handed duplex helices and of mirror symmetric (*L*-DNA) molecules, forming left-handed helices. Since the nematic ordering of DNA duplexes is mediated by their end-to-end aggregation into linear columns, by controlling the terminals of both enantiomers we could study the propagation of chirality in solutions where the *D* and *L* species form mixtures of homochiral columns, and in solutions of heterochiral columns. The two systems behave in markedly different fashion. By adopting a simple model based on nearest-neighbor interactions, we account for the different observed dependence of the chirality of these two systems on the enantiomeric ratio.

DOI: 10.1103/PhysRevLett.110.107801 PACS numbers: 61.30.Eb, 61.30.St, 87.15.Zg

In the last decades, modern statistical physics has made remarkable progress towards explaining an ever-broader range of distinct types of molecular ordering on the basis of the properties of their molecular constituents. A notable exception is the lack of a general theory for the prediction of how strongly the presence of chiral centers in molecules affects phase behavior and structure on mesoscopic length scales [1]. Even when the molecular shape is symmetric and very well known, such as the double helical shape of B-DNA, the cooperative effects of the molecular chirality are amazingly complex and hard to model [2–5]. The recent discovery of the liquid crystal chiral nematic (N^*) phase in solutions of ultrashort DNA double helices (down to 6 bases) [6] has offered new opportunities to explore this topic. In these nano DNA systems the formation of liquid crystal phases is mediated by the end-to-end aggregation of DNA duplexes into columns of chemically distinct but physically continuous duplexes. Transition to the N^* phase occurs when such weakly bound linear aggregates have a sufficiently large shape anisotropy which, according to recent modeling [7,8] and in the conditions so far explored, corresponds to about 10 stacked duplexes.

The combination of self-assembly and chirality opens a new possibility for the study of the propagation of chirality. While in typical lyotropic and thermotropic cholesterics the monomers have a fixed chirality given by the molecular or colloidal structure, the self-assembly of DNA can be exploited to tune the chirality of the columnar aggregates and study its effect on the collective ordering. Here we turn the exploration of DNA chirality in a new direction, mixing natural *D*-DNA oligomers and their *L*-DNA enantiomers having perfectly mirror symmetrical structures. Because of the enantioselectivity of Watson-Crick interactions [9,10], *L* and *D* nanooligomers do not bind. Thus, when self complementary *L* and *D* oligomers are put together in solution, a mixture of mirror symmetric right- and left-handed helices is obtained [11] [see Fig. 1(a)]. *L*-oligonucleotides are available because they have been clinically developed as so-called Spiegelmers, 3D structured oligomers that can survive in a biological environment because of their nonnative chirality, and yet are capable of binding and inhibiting pharmacologically relevant target molecules [12–14].

For this study we selected three variants of the ''Dickerson Dodecamer'' (DD), CGCGAATTCGCG, a self-complementary 12 base pair sequence forming canonical B-DNA duplexes [15]. When -OH terminated, DD forms blunt-ended duplexes. In this case, interduplex interactions are promoted by the stacking of the paired bases at the duplex terminals [6]. Recent atomistic simulations of this system [16] show that in the absence of terminal phosphates the helices are rather free to rotate around their axis, in a way that appears to depend on the structure of the duplex terminals only. This implies that (i) in homochiral solutions the stacked columns of duplexes do not in general preserve helical continuity, and (ii) since no chiral group is present in the flat polyaromatic surface formed by the paired nucleobases, we expect stacking forces to act similarly between duplexes of the same or different chirality, thus enabling the formation of heterochiral aggregates. A different behavior is expected when end-to-end interactions are mediated by the

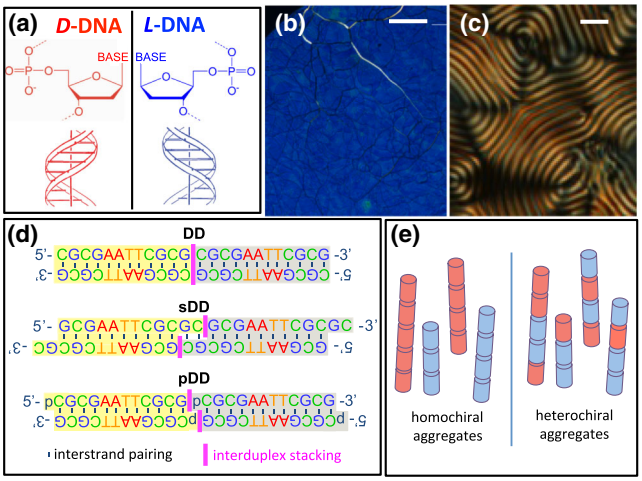

FIG. 1 (color online). (a) Natural D-deoxyribose and related right-handed D-DNA (red) and mirror-image L-deoxyribose with left-handed L-DNA (blue). (b), (c) Depolarized Transmitted Light Microscopy micrograph showing textures of the nematic phase of a L-pDD sample having a pitch of 0.3 μm (b) and of a DD sample with $r = 0.33$ having a pitch of 5.6 μm (c) The color in (b) is produced by selective reflection while the distance between bright fringes in (c) corresponds to half of the pitch. Size bars are 100 (b) and 10 μm (c). (d) Schematic representation of the end-to-end interactions between duplexes formed by the sequences considered in this work. Each duplex is marked by either yellow or gray shading. (e) Because of the selectivity of the pairing interactions, sDD is expected to form homochiral aggregates. On the other hand, DD and pDD enantiomeric duplexes can form heterochiral aggregates because the stacking interaction is not chirally selective.

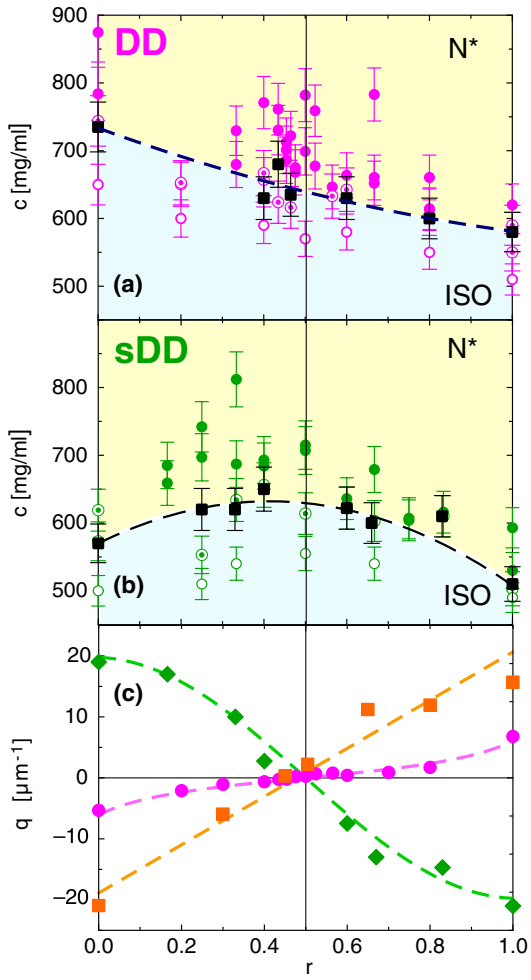

FIG. 2 (color online). (a), (b) Phase behavior of aqueous solutions of DD (a) and sDD (b) as a function of DNA concentration and enantiomeric ratio at fixed temperature ($T \sim 20\,^{\circ}$C). Symbols indicate the observed phase: nematic (full dots), isotropic (empty dots) and N^*-I phase coexistence (target dots). Black squares are samples at coexistence in which the nematic phase fills between 60 and 70% of the volume. The dashed black line marks the phase boundary $c_{I-N^*}(r)$ through the fit as described in the text. (c) pitch wave number $q = 2\pi/p$ as a function of the ratio r for the N^* phase of sDD (green diamonds), DD (pink dots) and pDD (orange squares). Data are relative to $T \sim 20\,^{\circ}$C and to samples in which the nematic phase fills between 60 and 70% of the volume. Experimental uncertainties are comparable to the symbol size. The dashed lines are best fits obtained by the model.

pairing of overhangs such as in the case of the "shifted-DD" sequence ("sDD", 5′-GCGAATTCGCGC-3′) that forms duplexes identical to DD except for having two unpaired, but mutually complementary, terminal bases [Fig. 1(d)] [17]. Differently from DD, (i) sDD homochiral duplexes aggregate as a continuous helix [18], and (ii) sDD duplexes of opposite chirality do not aggregate because of the enantioselectivity of Watson-Crick interactions which stabilize homochiral columnar aggregates relative to those of mixed chirality [Fig. 1(e)]. A possibly intermediate condition is provided by DD duplexes phosphorilated on the 5′ end (pDD). Once aggregated, DD, pDD, and sDD have the same overall sequence of bases [Fig. 1(d)].

DD, pDD, and sDD were synthesized in both D- and L-DNA form, by NOXXON Pharma AG. All samples were HPLC purified and counterions were exchanged into Na^+. Mixtures at various enantiomeric ratios $r = c_D/c$, where $c = c_D + c_L$ and c_D, c_L are the concentration of the two enantiomers, were prepared as detailed in the Supplemental Material [19]. After equilibration at room temperature ($T = 20\,^{\circ}$C) we measured c via microinterferometry [6]; see Figs. 1(b) and 1(c). The handedness H and pitch p of the chiral nematic phase have been determined through microscope-based analysis [19]. In this Letter H is expressed through the sign of p: $p > 0$ ($p < 0$) for RH (LH) N^* phases. We have found N^* ordering at all values of r, at concentrations that depend on r. Figures 2(a) and 2(b) show the c-r phase diagram for DD and sDD, respectively.

We fit the coexistence [black dots in Figs. 2(a) and 2(b)] data to $c_{I-N^*}(r) = \alpha + \beta(r - 0.5) + \gamma(r - 0.5)^2$ (black dashed lines). The linear term is due to different levels of sample purity, still present despite our efforts in treating the samples with uniform standard methods. The quadratic

term indicates the extent to which nematic ordering is promoted ($\gamma > 0$) or inhibited ($\gamma < 0$) in a 1:1 mixture relative to that of the pure enantiomers. For DD mixtures $\gamma \sim 0$, supporting the notion that the D and L duplexes mix ideally at all concentrations in the isotropic and nematic. On the contrary, in the case of sDD the quadratic term with $\gamma > 0$ is much larger, indicating that nematic ordering is disfavored in the mixtures.

Despite the asymmetry in the concentrations of the enantiomers, the chirality of N^* ordering of pure L-DNA species is mirror symmetric to the ones of D-DNA (Table I). Data in Table I confirm that chiral properties of pure D-DNA and pure L-DNA systems have a complex dependence on the oligomer sequence: the chirality of the N^* phase of DD and pDD is opposite to the one of sDD. Moreover, the chirality is larger for pDD and sDD oligos, both displaying a pitch matching the low-wavelength end of the visible spectrum, while p in the case of DD is larger. These results are in line to what we observed in the case of pure natural D-DNA. Indeed, variations in base-sequence and length having only minor effects on the DNA helical shape can strongly affect the chiral nature of the collective structures [20]. In part, this complex behavior may be the outcome of the competition between steric interactions, that in the case of D-DNA promote right-handed twist of the N^* phase, and electrostatic interactions, favoring the opposite handedness [21]. This notion appears to be in agreement with experimental observation [20,21] since sequences that form N^* phases at lower concentration, in which columns of duplexes are thus less often in close contact, adopt the handedness favored by electrostatic interactions.

Figure 2(c) shows the pitch wave number $q = 2\pi/p$ for the three mixed D and L systems, as a function of the enantiomer ratio. For each sequence we observed a reversal of the phase chirality progressively adding L-DNA to the natural one. Moreover, the dependence of q on r is different in the three cases: in the case of DD there is a larger dependence at small and large values of r, while the dependence is weak around $r = 0.5$, where the system is close to racemic; in the case of sDD the behavior is opposite. For pDD, the dependence of q on r is close to linear. The nonlinear q vs r dependence found for DD and sDD, appears to be a distinctive feature of self-assembled systems, since investigations of the N^* phase formed by enantiomeric mixtures both in the case of thermotropic [22] and lyotropic [23] systems are generally described by a linear dependence of q on r.

The chirality of the N^* phase is rooted in the pair interactions of the constituent molecules, which introduces an angular distortion in their otherwise parallel alignment. Such effect is usefully expressed through the chiral strength $k_T = (du/dq)_{q=0}$, u being the free energy density of the N^* phase. Upon envisioning the N^* phase as a stack of nematic sheets, k_T expresses the torque surface density acting between sheets that favors the twisting of the stack and may be positive or negative depending on the prevailing of the steric vs electrostatic interactions [21]. The amplitude of the resulting pitch is given by the balance between k_T and the twist elastic coefficient K_{22}, favoring the unwinding of the phase into a nonchiral nematic: $q = -k_T/K_{22}$ [21]. However, K_{22} is known to depend only weakly on the molecular length [24], as confirmed by recent experiments in the context of self-assembled chromonic liquid crystals [25]. Accordingly, in the following discussion we will assume that $q(c, r) \propto k_T(c, r)$.

In the simplest model, the dependence of k_T and q on r can be assumed to depend on the frequency of chiral contacts between neighboring columns, each contributing the same amount τ_0 to the chiral strength. We expect

$$k_T = \tau_0(c_D^2 - c_L^2) = \tau_0 c^2(2r - 1). \quad (1)$$

Equation (1) embodies the notion that D-D and L-L contacts produce torques of opposite sign and that, by symmetry, cross D-L contacts do not give rise to chiral coupling. Equation (1) is appropriate for enantiomer mixtures in which the chiral units are monodisperse and not self-assembled, as it is also confirmed by the resulting linear dependence of q on r [22,23]. However, the self-assembled nature of the systems here considered requires including further elements into the model. Contacts between columns are certainly not pointlike, but rather involve whole segments of the columns. The existence of such a longitudinal range ℓ is demonstrated by the markedly different pitch of DD and pDD in pure L or D systems. The two molecules differ only for the presence of the terminal phosphate, which provides pDD a good degree of helical continuity along the chemically discontinuous aggregated columns [16]. The localized helical discontinuities along the DD columns have thus an effect which is much larger than expected from the involved fraction of

TABLE I. Comparison of the handedness (RH or LH), pitch and concentration for N^*-I coexistence of solutions of pure natural D-DNA and enantiomeric L-DNA for the sequences studied in this work.

Sequence	Chirality of N^*	Pitch [μm]	$c_{I\text{-}N}$ [mg/ml]
DD	RH (D-DNA), LH (L-DNA)	$1(D)$, $-1.1(L)$	$580(D)$, $710(L)$
pDD	RH (D-DNA), LH (L-DNA)	$0.4(D)$, $-0.3(L)$	$560(D)$, $660(L)$
sDD	LH (D-DNA), RH (L-DNA)	$-0.30(D)$, $0.32(L)$	$520(D)$, $570(L)$

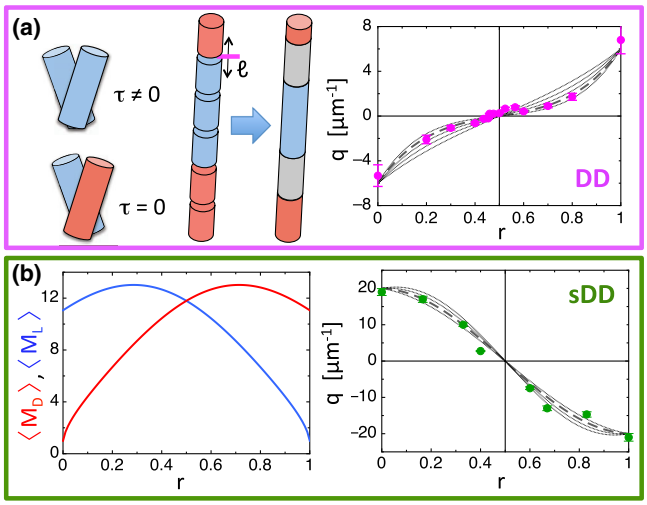

FIG. 3 (color online). (a) Interaction between two DNA duplexes of the same chirality (same color) give rise to a torsional contact ($\tau \neq 0$), producing a twist of given handedness. On the opposite, interaction between enantiomeric duplexes (different color) does not give rise to torque ($\tau = 0$). Inside heterochiral aggregates, regions closer than ℓ to L-D stacking planes have a weakened effect on the torque. We model this situation by picturing the column as formed by chiral (blue or red) regions and non-chiral (gray) regions. In the panel on the right we compare the q vs r data (pink dots) with model predictions for various values of ℓ (dotted lines): $\ell = 0.8$, $l = 1.6$, $l = 2.4$, $l = 3.2$, and $\ell = 4$ nm. The choice $\ell = 3.2$ nm (thick dashed line) appears to best approach the data. (b) Average aggregate length of D-DNA ($\langle M_D \rangle$, red line) and L-DNA ($\langle M_L \rangle$, blue line) as a function of r in sDD mixtures obtained using the values of r and c determined at coexistence. In the panel on the right we compare the q vs r data (green dots) with the model predictions obtained with different values of the cutoff length s (dotted lines): $s = 0$, $s = 2$, $s = 4$, and $s = 6$. The choice $s = 2$ (thick dashed line) appears to best approach the data.

bases (2 out of 12), but reasonable if the interaction is spread on a range. In columns where D and L duplexes are mixed, the presence of a longitudinal interaction range smears the local chirality and reduces the overall chiral strength of the aggregates. We have included this notion in the model (i) by assuming random L vs D sequences along the columns and (ii) by assuming that whenever there are two consecutive duplexes of opposite handedness within a column, there is range of nonchiral interactions extending from their contacting terminals for a length ℓ, as sketched in Fig. 3(a).

Accordingly, a collision between two columns that brings two D-DNA duplexes in contact contributes to the chiral strength only if the point of closest contact is farther than ℓ from any D-L stacking plane. When these notions are inserted in the computation of k_T, a family of curves having the same curvature of the experiments is obtained by varying ℓ as shown in Fig. 3(a) (more details in Ref. [19]). The choice $\ell = 3.2$ nm produces the best matching with the data. This is a realistic value, of the order of the width of DNA double helices, which is about 2 nm. However, ℓ is expected to depend significantly on the persistence length of the aggregates, a quantity not yet experimentally accessible.

A different scenario is instead obtained in the sDD mixtures where homochiral columns are formed, and thus where the correction depending on the interaction length is not appropriate. In this case, duplexes of one parity are "diluted" by their enantiomers with which they do not aggregate. Therefore, the mean number of monomers $\langle M_D \rangle$ and $\langle M_L \rangle$ forming the D and L columns depend differently on c_D and c_L. By adopting a simple extension of the model in Refs. [8,19], we can compute $\langle M_D \rangle$ ($\langle M_L \rangle$) as a function of c_D (c_L), the concentration of the aggregating monomers, and of c. The total DNA concentration promotes the lengthening of both $\langle M_D \rangle$ and $\langle M_L \rangle$ through excluded volume interactions, insensitive, to a first order consideration, to handedness. Figure 3(b) shows $\langle M_D \rangle$ and $\langle M_L \rangle$ expected from the values of r and c determined at coexistence [dashed line in Fig. 2(b)]. Further details on the calculation are given in Ref. [19]. Therefore, in strongly unbalanced mixtures where $r \approx 0$, $\langle M_D \rangle \ll \langle M_L \rangle \approx$ const. Dual behavior is found at the other extreme, $r \approx 1$. In these regions, we expect that the effect on the chiral strength of the minority enantiomers is less than expected on the basis of the total concentration because of the difference in the aggregate length. Shorter aggregates yield a reduced contribution to the phase chirality both because the proximity to the column terminals weakens the interactions (for the same longitudinal interaction range discussed above), and because shorter aggregates are intrinsically more disordered [8] and hence have a weaker angular drag on the whole phase. We have incorporated this notion into the model by inserting a cutoff s such that when contacts involve columns shorter than s, they do not contribute to the chiral strength. This assumption leads to the family of curves shown in Fig. 3(b) (details in Ref. [19]), having the same curvature of the sDD data. Choices with $2 < s < 4$ produce the best match with the data. Coherently with the model assumptions, the value obtained for s is much shorter than the average aggregate length.

In Fig. 2(c) we also show the dependence of the pitch wave number of pDD on r (red squares). The phosphate termination of pDD certainly has an effect on the end-to-end stacking [16], thus making the aggregates of this system somewhere in between the random DD and the homochiral sDD columns. Accordingly, the nearly linear q vs r dependence can be understood as being in between the opposite curvatures of DD and sDD systems (more discussion in Ref. [19]).

The possibility offered by the self-assembly of DNA nanolength duplexes was exploited here to produce systems in which the local interaction between pairs of molecules was maintained the same, while their distribution

within aggregates was controllably modified. This enabled us to disregard the difficult problem of determining the torque resulting from pair interactions, a topic of current investigation [21], while focusing on the mechanisms of its propagation to the phase behavior. The success of the simple models here employed, based on nearest-neighbor interactions, indicates that all the difficulties in interpreting the nematic ordering of chiral molecules are actually nested in the determination of the torque resulting from pair interactions, while its effect on the phase can be satisfactorily accounted for by a simple approach.

This work was supported by the Grant PRIN Program of the Italian MIUR Ministry and by the NSF MRSEC Grant No. DMR 0820579 and NSF Grant No. DMR 1270606. We thank Dr. Lucas Bethge and the chemical group of NOXXON for providing the oligonucleotides, and Dr. Alberta Ferrarini, Elisa Frezza, Tommaso Fraccia, Fabio Giavazzi and Cristiano De Michele for stimulating discussions.

[1] H. G. Kuball and T. Höfer, *Partially Ordered Systems* (Springer-Verlag, New York, 2001), p. 67.
[2] A. A. Kornyshev, D. Lee, S. Leikin, and A. Wynveen, Rev. Mod. Phys. **79**, 943 (2007).
[3] N. Katsonis, E. Lacaze, and A. Ferrarini, J. Mater. Chem. **22**, 7088 (2012).
[4] A. G. Cherstvy, Phys. Chem. Chem. Phys. **13**, 9942 (2011).
[5] H. H. Wensink and G. Jackson, J. Chem. Phys. **130**, 234911 (2009).
[6] M. Nakata, G. Zanchetta, B. D. Chapman, C. D. Jones, J. O. Cross, R. Pindak, T. Bellini, and N. A. Clark, Science **318**, 1276 (2007).
[7] T. Kuriabova, M. D. Betterton, and M. A. Glaser, J. Mater. Chem. **20**, 10 366 (2010).
[8] C. De Michele, T. Bellini, and F. Sciortino, Macromolecules **45**, 1090 (2012).
[9] D. D'Alonzo, A. Guaragna, and G. Palumbo, Chem. Biodiversity **8**, 373 (2011).
[10] A. Garbesi, M. L. Capobinanco, F. P. Colonna, L. Tondelli, F. Arcamone, G. Manzini, C. W. hilbers, J. M. E. Aelen, and M. J. J. Blommers, Nucleic Acids Res. **21**, 4159 (1993).
[11] M. Vallazza, M. Perbandt, S. Klussmann, W. Rypniewski, H. M. Einspahr, V. A. Erdmann, and Ch. Betzel, Acta Crystallogr. Sect. D **60**, 1 (2004).
[12] S. Klussman, A. Nolte, R. Bald, V. A. Erdmann, and J. P. Fürste, Nat. Biotechnol. **14**, 1112 (1996).
[13] D. Eulberg, W. Purschke, H. J. Anders, N. Selve, and S. Klussmann, *Spiegelmer NOX-E36 for Renal Diseases* (Jens Kurreck, RSC, 2008).
[14] A. Ellington and J. Szostak, Nature (London) **346**, 818 (1990).
[15] R. Wing, H. Drew, T. Takano, C. Broka, S. Tanaka, K. Itakura, and R. E. Dickerson, Nature (London) **287**, 755 (1980).
[16] C. Maffeo, B. Luan, and A. Aksimentiev, Nucleic Acids Res. **40**, 3812 (2012).
[17] G. Zanchetta, M. Nakata, M. Buscaglia, N. A. Clark, and T. Bellini, J. Phys. Condens. Matter **20**, 494214 (2008).
[18] H. M. Berman, Biopolymers **44**, 23 (1997).
[19] See Supplemental Material at http://link.aps.org/supplemental/10.1103/PhysRevLett.110.107801 for sample preparation, characterization of the chiral nematic phase and for the description of the models of chiral propagation.
[20] G. Zanchetta, F. Giavazzi, M. Nakata, M. Buscaglia, R. Cerbino, N. A. Clark, and T. Bellini, Proc. Natl. Acad. Sci. U.S.A. **107**, 17 497 (2010).
[21] E. Frezza, F. Tombolato, and A. Ferrarini, Soft Matter **7**, 9291 (2011).
[22] D. K. Yang and P. P. Crooker, Phys. Rev. A **35**, 4419 (1987).
[23] E. Barry, D. Beller, and Z. Dogic, Soft Matter **5**, 2563 (2009).
[24] M. A. Osipov and S. Hess, Mol. Phys. **78**, 1191 (1993).
[25] S. Zhou *et al.*, Phys. Rev. Lett. **109**, 037801 (2012).